



Phase-field study on competition precipitation process of Ni–Al–V alloy

Yan-li LU, Guang-ming LU, De-wei JIA, Zheng CHEN

State Key Laboratory of Solidification Processing, Northwestern Polytechnical University, Xi'an 710072, China

Received 17 March 2014; accepted 23 June 2014

Abstract: With microscopic phase-field kinetic model, atomic-scale computer simulation program for the precipitation sequence and microstructure evolution of the ordered intermetallic compound γ' and θ in ternary $\text{Ni}_{75}\text{Al}_x\text{V}_{25-x}$ alloy were studied. The simulation results show that Al concentration has important effects on the precipitation sequence. When Al concentration in $\text{Ni}_{75}\text{Al}_x\text{V}_{25-x}$ alloy is low, $\theta(\text{Ni}_3\text{V})$ ordered phase will be firstly precipitated, followed by $\gamma'(\text{Ni}_3\text{Al})$ ordered phase. With Al concentration increasing, θ and γ' ordered phases are simultaneously precipitated. With Al concentration further increasing, γ' ordered phase is firstly precipitated, followed by θ ordered phase. There is a competition relationship between θ and γ' ordered phases during growth and coarsening process. No matter which first precipitates, θ ordered phase always occupies advantage in the competition process of coarsening, thus, the microstructure with preferred orientation is formed.

Key words: Ni–Al–V alloy; microstructure evolution; precipitation process; phase-field method

1 Introduction

The Ni_3X intermetallic compounds have attracted considerable interests as the high temperature structural materials and as a component in composite because of their good resistance against high temperature creep [1,2]. The morphology, size and distribution of Ni_3X intermetallic compound have important effects on the mechanical properties of superalloys [3,4]. NABARRO et al [5] predicted the microstructure with preferred orientation in superalloys by calculating the thermodynamic driving force. REED et al [6] studied the relation between the directional γ' phase and strain rates. LI et al [7] studied the influence of pre-compression on the directional γ' phase. WU et al [8] observed the microstructure evolution of a Ni_3Al -based single crystal superalloy. Unfortunately, these experiments are usually limited to a small observation range, and cannot observe the microstructure evolution at atomic scale.

The microscopic phase-field kinetic model [9–11] based on the Ginzburg–Landau kinetic equation is an effective method to study the precipitation process, in which it is not necessary to assume the phase structure or the precipitation style, and the growth and coarsening process can be modeled simultaneously. In the last

several years, many efforts have been made to study the microstructure evolution using phase-field method. ZHANG et al [12] expounded the site occupation evolution of alloying element in Ni–Al–V alloy. YANG et al [13] studied the transformation of rafting style in $\text{Ni}_{75}\text{Al}_{8.5}\text{V}_{16.5}$ alloy. However, the effect of solute concentration and competitive relation between two phases on the microstructure evolution has not been investigated yet. In the present work, the effect of Al concentration on the microstructure evolution of phase growth and coarsening in $\text{Ni}_{75}\text{Al}_x\text{V}_{25-x}$ alloy (x represents Al concentration) was investigated. The morphological evolution, precipitate sequence, and volume fraction during the precipitation process were mainly analyzed.

2 Theoretical modeling

2.1 Microscopic phase-field kinetic model of ternary system

The microscopic phase-field kinetic model is based on the Onsager and Ginzburg–Landau equation [14,15], which describes the atomic structure morphology by single-site occupation probability. $P_A(\mathbf{r}, t)$, $P_B(\mathbf{r}, t)$ and $P_C(\mathbf{r}, t)$ respectively represent the probabilities of finding A, B or C atom at a given site and a given time. Since only two equations are independent at each lattice

site, and there will be two independent kinetic equations at each lattice site for A and B, the microscopic phase-field kinetic model of ternary system is described as follows [16]:

$$\begin{cases} \frac{dP_A(\mathbf{r},t)}{dt} = \frac{1}{k_B T} \sum_{\mathbf{r}'} [L_{AA}(\mathbf{r}-\mathbf{r}') \frac{\partial F}{\partial P_A(\mathbf{r}',t)} + \\ L_{AB}(\mathbf{r}-\mathbf{r}') \frac{\partial F}{\partial P_B(\mathbf{r}',t)}] + \xi(\mathbf{r},t) \\ \frac{dP_B(\mathbf{r},t)}{dt} = \frac{1}{k_B T} \sum_{\mathbf{r}'} [L_{BA}(\mathbf{r}-\mathbf{r}') \frac{\partial F}{\partial P_A(\mathbf{r}',t)} + \\ L_{BB}(\mathbf{r}-\mathbf{r}') \frac{\partial F}{\partial P_B(\mathbf{r}',t)}] + \xi(\mathbf{r},t) \end{cases} \quad (1)$$

where $L_{\alpha\beta}(\mathbf{r}-\mathbf{r}')$ is a constant related to the exchange probabilities of a pair of atoms, α and β , at lattice site γ and γ' per unit time, and $\alpha, \beta=A, B, \text{ or } C$; k_B is the Boltzmann constant; $\xi(\mathbf{r}, t)$ is the thermal noise term, which is assumed to be Gaussian-distributed with the average value of zero, and is uncorrelated with space and time, and obeys the so-called fluctuation dissipation theory; F is the total free energy including the elastic strain energy contribution. Based on the mean-field approximation, F is given by the following equation:

$$\begin{aligned} F = & -\frac{1}{2} \sum_{\mathbf{r}} \sum_{\mathbf{r}'} [V_{AB}(\mathbf{r}-\mathbf{r}') P_A(\mathbf{r}) P_B(\mathbf{r}') + \\ & V_{BC}(\mathbf{r}-\mathbf{r}') P_B(\mathbf{r}) P_C(\mathbf{r}') + V_{AC}(\mathbf{r}-\mathbf{r}') P_A(\mathbf{r}) P_C(\mathbf{r}')] + \\ & k_B T \sum_{\mathbf{r}} [P_A(\mathbf{r}) \ln(P_A(\mathbf{r})) + P_B(\mathbf{r}) \ln(P_B(\mathbf{r})) + \\ & P_C(\mathbf{r}) \ln(P_C(\mathbf{r}))] \end{aligned} \quad (2)$$

where $V_{\alpha\beta}(\mathbf{r}-\mathbf{r}')$ is the interaction energy between α and β at lattice site γ and γ' , including short-range chemical interaction $V_{\alpha\beta}(\mathbf{r}-\mathbf{r}')_{\text{ch}}$ and long-range strain-induced elastic interaction $V_{\alpha\beta}(\mathbf{r}-\mathbf{r}')_{\text{el}}$:

$$V_{\alpha\beta}(\mathbf{r}-\mathbf{r}') = V_{\alpha\beta}(\mathbf{r}-\mathbf{r}')_{\text{ch}} + V_{\alpha\beta}(\mathbf{r}-\mathbf{r}')_{\text{el}} \quad (3)$$

Here, the fourth nearest-neighbor interatomic model was employed, and the data of interatomic interchange energies were taken from Ref. [16].

2.2 Microelasticity theory

In the microelasticity theory, the elastic strain energy of solid solution is given as a sum of two physically distinct terms [17]: 1) the configuration-independent term describing the self-energy and image force-induced energy; 2) the configuration dependent term associated with the concentration inhomogeneity. The first term is not affected by spatial redistribution of solute atoms and therefore it can be ignored. The second term, however, gives a substantially nonlocal elastic strain energy change associated with spatial distribution of solute atoms, so, it affects the morphology of the precipitation phase.

In a real space, the configuration-dependent elastic strain energy associated with an arbitrary atomic distribution $P(\mathbf{r})$ can be described as [18]

$$E_{\text{el}} = -\frac{1}{2} \sum_{\mathbf{r}'} V_{\alpha\beta}(\mathbf{r}-\mathbf{r}')_{\text{el}} P_{\alpha}(\mathbf{r}) P_{\beta}(\mathbf{r}') \quad (4)$$

The Fourier transformation of Eq. (4) yields

$$E_{\text{el}} = -\frac{1}{2N} \sum_{\mathbf{k}} V(\mathbf{k})_{\text{el}} |P(\mathbf{k})|^2 \quad (5)$$

where N is the total lattice number. The prime in the Eq. (5) implies that the point $k=0$ is excluded. $V(\mathbf{k})_{\text{el}}$ is the Fourier transformation of the density function of elastic energy, and the long-wave approximation for $V(\mathbf{k})_{\text{el}}$ can be described as

$$V_{\alpha\beta}(\mathbf{k})_{\text{el}} \approx B(\mathbf{e}) = B(n_x^2 n_y^2 - \frac{1}{8}) \quad (6)$$

where $\mathbf{n}=\mathbf{k}/k$ is a unit vector in the \mathbf{k} direction; n_x and n_y are components of the unit vector \mathbf{k} along the x and y axes, therefore, $V_{\alpha\beta}(0)_{\text{el}} \approx -B/8$; B is the strain energy parameter which characterizes the elastic properties and the crystal lattice mismatch,

$$B = -\frac{4(C_{11} + 2C_{12})^2}{C_{11}(C_{11} + C_{12} + 2C_{44})} \varepsilon_0^2 \delta \quad (7)$$

where $\varepsilon_0=da(c)/(a_0dc)$ is the concentration coefficient of crystal lattice expansion caused by the atomic size difference; $a(c)$ is the crystal lattice parameters of solute; a_0 is the crystal lattice parameters of matrix; c is the atomic fraction of solute; $\delta=C_{11}-C_{12}-2C_{44}$ is the elastic anisotropy constant and C_{ij} is the elastic constants of Ni-based solid solution. In this study, $C_{11}=206.8$ MPa, $C_{12}=148.5$ MPa, $C_{44}=94.4$ MPa were chosen based on the value of Ni-based alloy at 1050 K [19].

In this simulation, Eq. (1) was solved in the reciprocal space by taking Fourier transformation to simplify the solution process. Finally, the clear atomic configuration and phase morphology of the growth and coarsening process could be obtained, and the relationship between atomic occupation probability and time was acquired as well.

3 Results and discussion

The $\text{Ni}_{75}\text{Al}_x\text{V}_{25-x}$ alloys ($x=4, 5.5, 10$) aged at 1050 K are located in the $\gamma'+\theta$ region [20,21], both γ' (Ni_3Al , $L1_2$) and θ (Ni_3V , DO_{22}) ordered phase can be precipitated from the matrix during the precipitation process. The simulated pictures are two-dimensional projection along [010] direction and are depicted with different colors. If the occupation probability of vanadium is 1.0, its sublattice is red. If the occupation probability of aluminum is 1.0, the sublattice is green. Therefore, the θ phase appears to be red and the γ' phase

appears to be green, and all the nickel sublattices in both phases appear to be blue. The ordered phase structures are shown in Fig. 1. The simulation was performed in a square lattice consisting of 128×128 unit cells, and the periodic boundary conditions were applied along both dimensions. The time step (Δt) was 0.0001.

3.1 Microstructure evolution of phase growth

The microstructure evolution of phase growth in $\text{Ni}_{75}\text{Al}_x\text{V}_{25-x}$ alloy ($x=4.0, 5.5, 10.0$) is shown in Fig. 2. For $\text{Ni}_{75}\text{Al}_4\text{V}_{21}$ alloy, the concentration of disorder matrix begins at 500 time step, as shown in Fig. 2(a1). With the increase of atomic occupation probability at each site, it can be observed that the first precipitate is θ phase, as shown in Fig. 2(a2). With increase in time, θ phase grows bigger and γ' phase begins to precipitate along the phase boundary of θ , as shown in Figs. 2(b2–d2). With Al concentration increasing, for $\text{Ni}_{75}\text{Al}_{5.5}\text{V}_{19.5}$ alloy, θ and γ' phases are simultaneously precipitated from the disordered matrix, and then gradually grow up, as shown in Figs. 2(a2–d2). With Al concentration further increasing, for $\text{Ni}_{75}\text{Al}_{10}\text{V}_{15}$ alloy, γ' phase is firstly precipitated from the disordered matrix and it is separated by disorder area. With time proceeding, γ' phase grows bigger and bigger, and the width of disorder area among them decreases, as shown in Figs. 2(a3–b3). At about 10000 time step, θ phase begins to precipitate around the phase boundary of γ'

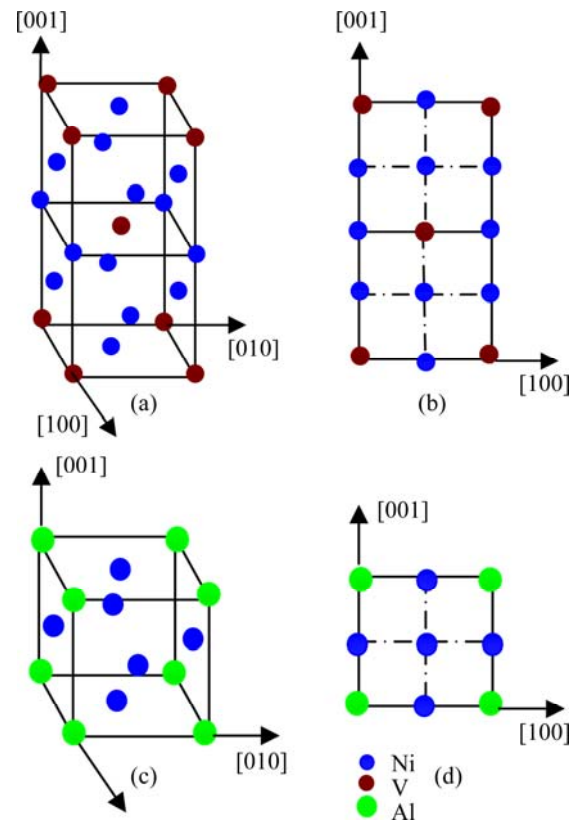


Fig. 1 Ordered phase structures: (a) θ phase (DO_{22}) crystal structure; (b) Projection of θ phase (DO_{22}); (c) γ' phase (L_{12}) crystal structure; (d) Projection of γ' phase (L_{12})

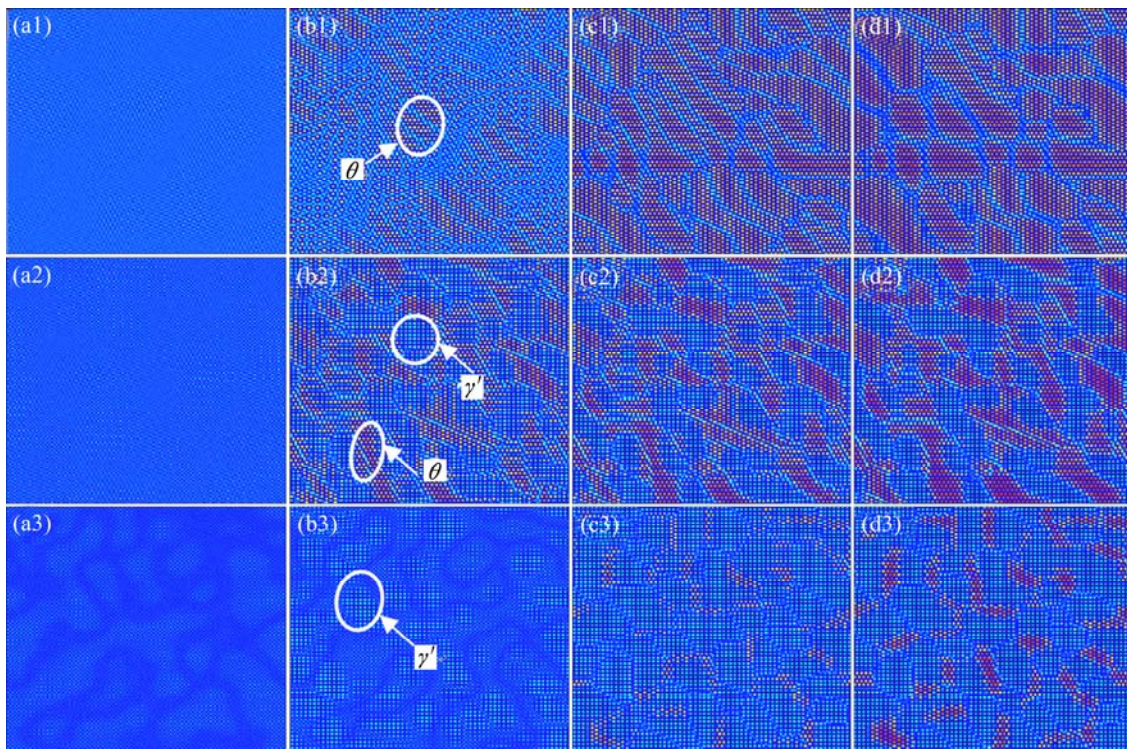


Fig. 2 Microstructure evolution of phase growth in $\text{Ni}_{75}\text{Al}_x\text{V}_{25-x}$ alloy: (a1) $x=4, t=500$; (b1) $x=4, t=2000$; (c1) $x=4, t=10000$; (d1) $x=4, t=15000$; (a2) $x=5.5, t=500$; (b2) $x=5.5, t=2000$; (c2) $x=5.5, t=10000$; (d2) $x=5.5, t=15000$; (a3) $x=10, t=500$; (b3) $x=10, t=2000$; (c3) $x=10, t=10000$; (d3) $x=10, t=15000$

phase, as shown in Fig. 2(c3). In the subsequent precipitation process, θ phase constantly grows up and some of γ' phase begins to dissolve, as shown in Fig. 2(d3). For $\text{Ni}_{75}\text{Al}_x\text{V}_{25-x}$ alloy ($x=4, 5.5, 10$), in the growth process, the distribution of θ and γ' phases is always irregular.

Figure 3 shows the variation of volume fraction of θ and γ' phases in $\text{Ni}_{75}\text{Al}_x\text{V}_{25-x}$ alloy ($x=4, 5.5, 10$). From Fig. 3(a), it can be seen that the volume fraction of θ phase firstly begins to increase after a period incubation period while that of γ' phase still remains at zero. When the volume fraction of θ phase reaches the equilibrium

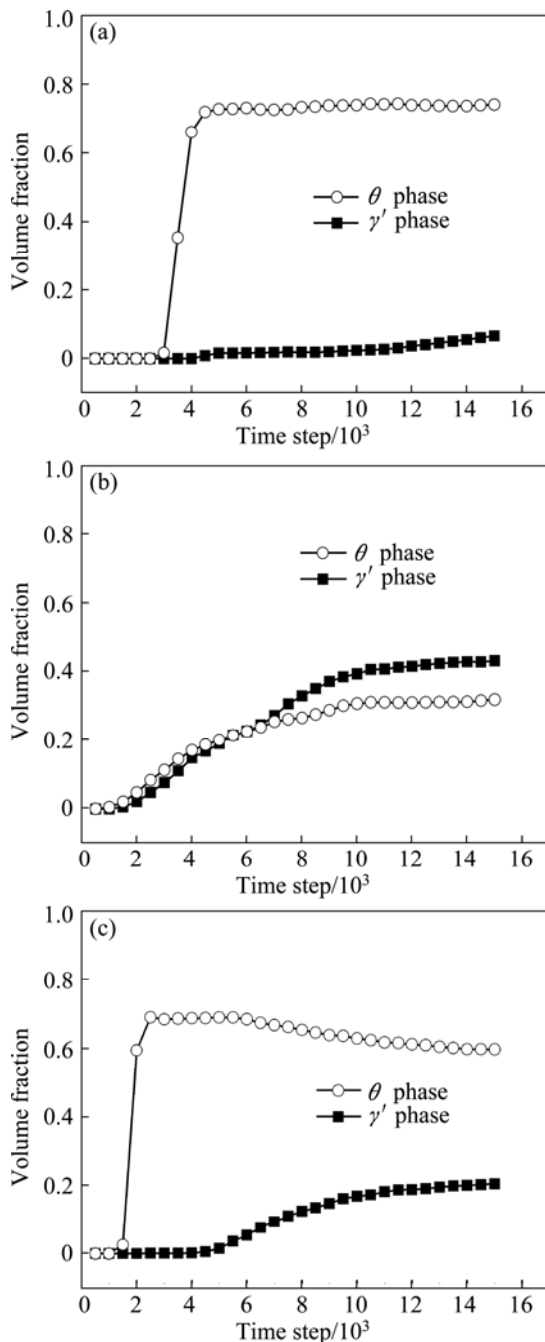


Fig. 3 Variation of volume fraction of θ and γ' phases in $\text{Ni}_{75}\text{Al}_x\text{V}_{25-x}$ alloy: (a) $x=4$; (b) $x=5.5$; (c) $x=10$

value, the volume fraction of γ' phase begins to increase, which indicates that θ phase is firstly precipitated, followed by γ' phase in $\text{Ni}_{75}\text{Al}_4\text{V}_{21}$ alloy. From Fig. 3(b), the volume fractions of θ and γ' phase simultaneously increase in $\text{Ni}_{75}\text{Al}_{5.5}\text{V}_{19.5}$ alloy after a period of incubation period. At the beginning, the volume fraction of θ phase increases faster than that of γ' phase, then the volume fraction of γ' phase exceeds that of θ phase. From Fig. 3(c), one can observe that the volume fraction of γ' phase in $\text{Ni}_{75}\text{Al}_{10}\text{V}_{15}$ alloy firstly increases rapidly to the maximum and declines slightly, due to the dissolution of some γ' phase at its phase boundary. At about 4800 time step, the volume fraction of θ phase begins to increase, which shows that θ phase is precipitated from the disordered matrix.

For $\text{Ni}_{75}\text{Al}_x\text{V}_{25-x}$ alloy, Al concentration decides the precipitation sequence of θ and γ' phases [20]. γ' phase is face-centered cubic structure which is isotropic, so it will not produce preferred growth at the free state. θ phase is a long-period and anisotropic structure (Fig. 1), and it mainly grows along its short axis ($[100]$ direction as shown in Fig. 1). When θ phase is first precipitated, the number of γ' phase is small at the early stage of precipitation process. Al atoms needed for γ' phase growth are mainly from phase boundary, and V atoms needed for θ phase are mainly from other θ phase. As we know, the atom diffusion rate at phase boundary is higher than that at phase inside, so, γ' phase occupied growth advantage at the early stage of precipitation process.

3.2 Microstructure evolution of phase coarsening

The microstructure evolution of phase coarsening is shown in Fig. 4. During the process of phase coarsening, some precipitates dissolve and others grow up. The shapes of θ and γ' phase change from initial irregular shape to quadrate. At the same time, their alignment becomes more and more regular, and some precipitates located in particular direction gradually grow and others disappear. In the later stage, θ and γ' phases exhibit quadrate shape and distribute regularly along the soft directions ($[100]$ and $[001]$ direction). The reason is that θ phase possesses advantage in the process of coarsening competition, which results in its preferred orientation.

In order to further identify the competition process, the average occupation probability of atom at different phases was calculated with the advantage of computer simulation, which is difficult to achieve by experiments, and presents the advantages of phase-field method.

Figure 5 shows the variation of atomic average occupation probability (OP) in θ and γ' phases of $\text{Ni}_{75}\text{Al}_x\text{V}_{25-x}$ ($x=4$). As the first precipitated phase is θ phase, the average OP of V atom in θ phase increases to the equilibrium value after the initial fluctuation. At the same time, θ phase contains a certain amount of Al

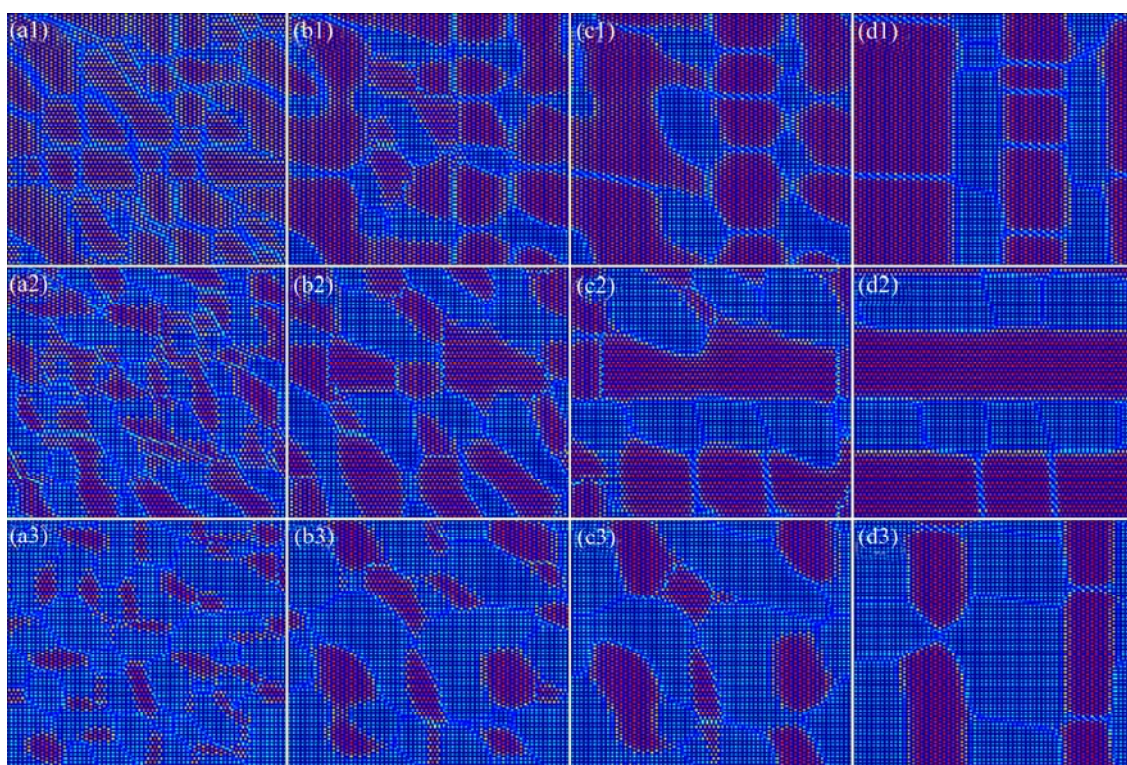


Fig. 4 Microstructure evolution of phase growth in $\text{Ni}_{75}\text{Al}_x\text{V}_{25-x}$ alloy: (a1) $x=4$, $t=18000$; (b1) $x=4$, $t=50000$; (c1) $x=4$, $t=150000$; (d1) $x=4$, $t=300000$; (a2) $x=5.5$, $t=18000$; (b2) $x=5.5$, $t=50000$; (c2) $x=5.5$, $t=150000$; (d2) $x=5.5$, $t=300000$; (a3) $x=10$, $t=18000$; (b3) $x=10$, $t=50000$; (c3) $x=10$, $t=150000$; (d3) $x=10$, $t=300000$

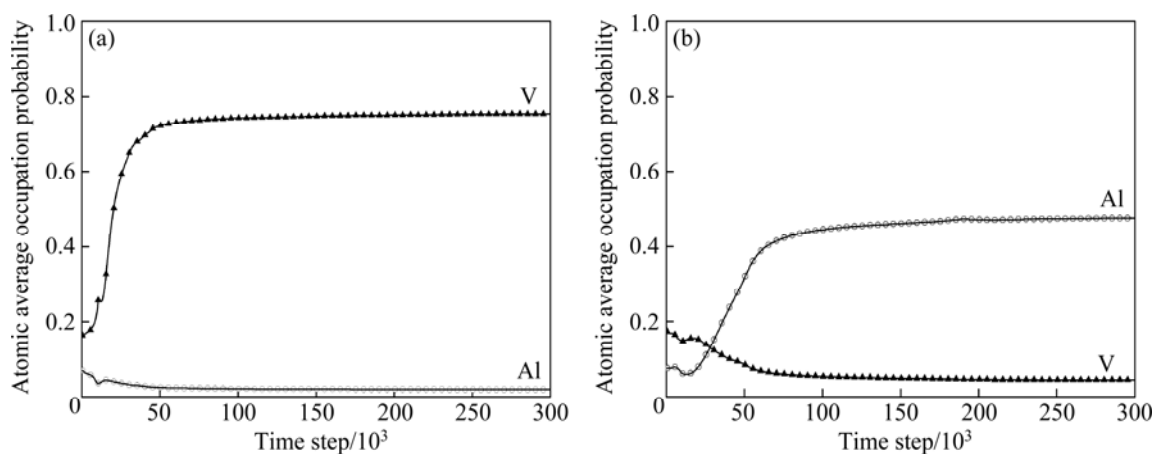


Fig. 5 Variation of atomic average occupation probability with time in different phase of $\text{Ni}_{75}\text{Al}_4\text{V}_{21}$ alloy: (a) θ phase; (b) γ' phase

atoms, which decreases to the equilibrium value, as shown in Fig. 5(a). When the average OP of V and Al atoms in θ phase reaches the equilibrium value, that of Al and V atoms in γ' phase is still in the change of stage, as shown in Fig. 5(b). At the later stage, the average OP of V atom in θ phase is larger than that of Al atom in γ' phase. The atomic average OP in θ phase relatively early reaches the equilibrium value, at this time, the variation of atomic average OP in γ' phase does not end, and the atomic migration causes further morphology evolution. When the atomic average OP in γ' phase reaches the

equilibrium state, there are still a number of V atoms but a very small number of Al atoms in θ phase when the atom average OP gets to the equilibrium state. So, during the coarsening process, the number of θ phase can supply V atom for coarsening of other θ phases, but cannot supply enough Al atom for the coarsening of other γ' phases. Thus, it can be indicated that Al atom required by the growth and coarsening of γ' phase is mainly from the dissolving of other γ' phases, and V atom required by the growth and coarsening of θ phase is from the dissolving of either other θ phases or other γ' phases. Therefore, the

coarsening rate of θ phase is greater than that of γ' phase, that is, the θ phase occupies advantage during coarsening process. At the later stage, θ and γ' phases align along [100] and [001] directions.

Due to the difference of solute V and Al atoms, there is difference of chemical energy for different precipitates, and the directional growth of θ phase along its short axis promotes the appearance of chemical energy anisotropy for different phases, causing the directional growth of γ' phase. CHENG et al [21] studied the influence of local chemical segregation on the directional coarsening of precipitates, and they concluded that internal chemical gradients which resulted from multiple alloying elements, could lead to the development of the preferred precipitates by leading to anisotropy in their growth kinetics during coarsening process. Our simulation results have a good agreement with those of CHENG et al [21] and TAKEYAMA KIKUCHI [22], which proves that the simulation result is believable.

The variation of atomic average OP in θ and γ' phases of $\text{Ni}_{75}\text{Al}_x\text{V}_{25-x}$ ($x=5.5$) is shown in Fig. 6. θ and γ' phases are almost simultaneously precipitated from disordered matrix. The change law of curve is similar to that of $\text{Ni}_{75}\text{Al}_x\text{V}_{25-x}$ ($x=5.5$). The atomic average OP of V

atom in θ phase reaches the equilibrium value faster than Al atom in γ' phase, which shows that θ phase occupies growth advantage in the competition process.

Figure 7 shows the variation of atomic average OP in θ and γ' phases of $\text{Ni}_{75}\text{Al}_x\text{V}_{25-x}$ ($x=10$). The first precipitate is γ' phase. When the average OP of Al and V atoms in γ' phase reaches the equilibrium value, the average OP of V and Al atoms in θ phase still changes, which indicates that the number and morphology of precipitates still change. At the equilibrium state, the average OP of V atom in θ phase is higher than that of Al atom in γ' phase. However, the average OP of Al atom in θ phase is lower than that of V atom in θ phase. Similar to that of $\text{Ni}_{75}\text{Al}_x\text{V}_{25-x}$ ($x=4, 5.5$), θ phase still possesses growth advantage in the competition process.

4 Verification

The simulated morphology of γ' phase in $\text{Ni}_{75}\text{Al}_8\text{V}_{17}$ alloy aged at 1023 K is shown in Fig. 8(a). The experiment observation [23] of γ' phase in Ni–8%Al–6%Ti (mole fraction) alloy aged at 1023 K for 1.728×10^5 s is shown in Fig. 8(b). From the comparison, it can be found that the simulation results are available.

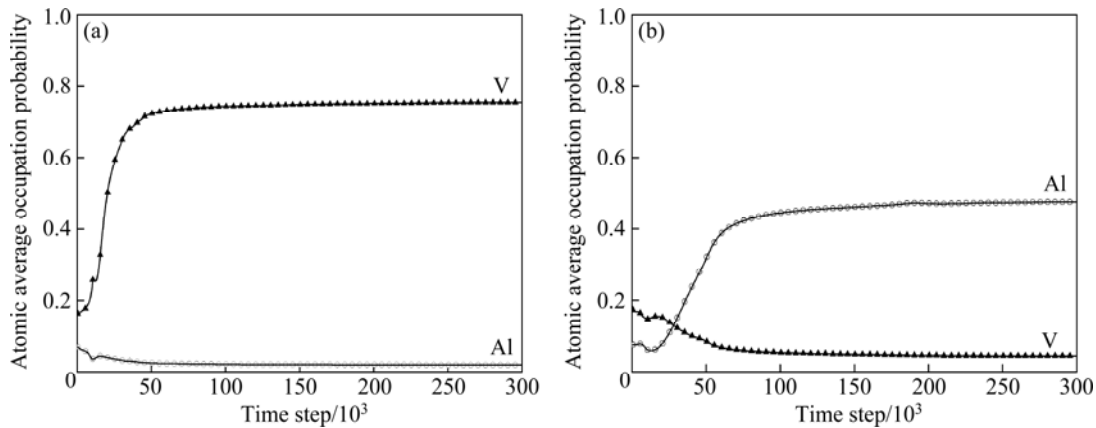


Fig. 6 Variation of atomic average occupation probability with time for different phases of $\text{Ni}_{75}\text{Al}_{5.5}\text{V}_{19.5}$ alloy: (a) θ phase; (b) γ' phase

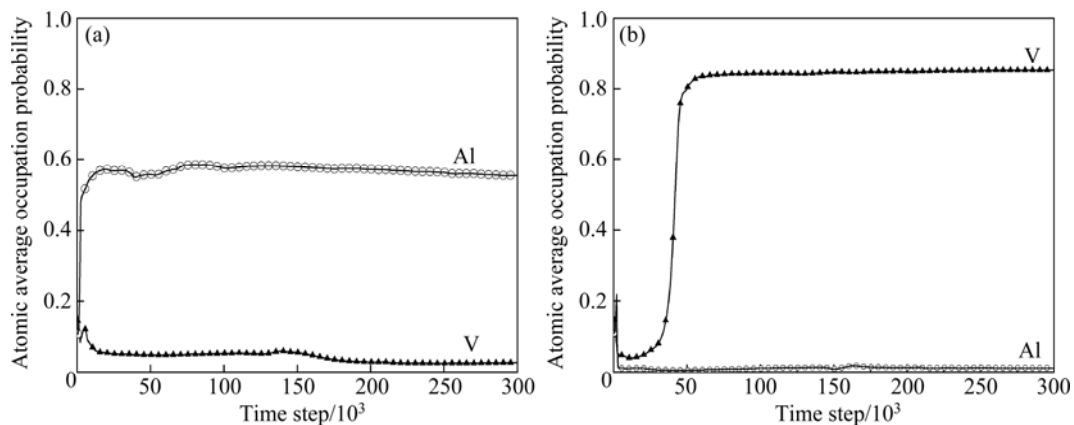


Fig. 7 Variation of atomic average occupation probability with time for different phases of $\text{Ni}_{75}\text{Al}_{10}\text{V}_{15}$ alloy: (a) γ' phase; (b) θ phase

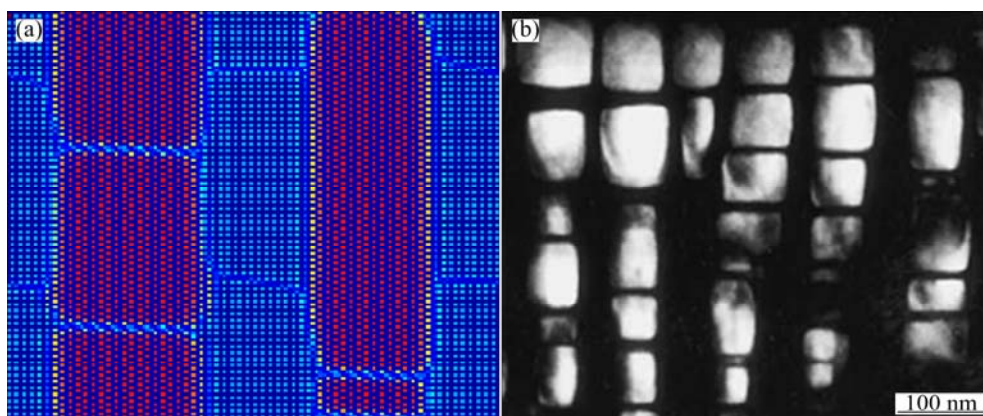


Fig. 8 Comparing γ' morphology obtained from simulated result (a) with experiment observation (b) [23]

5 Conclusions

1) The microstructure evolution of the ordered intermetallic compound γ' and θ in ternary $\text{Ni}_{75}\text{Al}_x\text{V}_{25-x}$ alloy during phase growth and coarsening in $\text{Ni}_{75}\text{Al}_x\text{V}_{25-x}$ ($x=4, 5.5, 10$) alloy was studied using microscopic phase-field kinetic model. The variation of atomic average OP and volume fraction for different precipitated phases was obtained.

2) The precipitation sequence is affected by Al concentration. For alloy with lower Al concentration, the first precipitated phase is θ phase. For alloy with medium Al concentration, θ and γ' phases are simultaneously precipitated from disordered matrix. For alloy with higher Al concentration, the first precipitated phase is changed to γ' phase.

3) During precipitation process, θ phase always occupies advantage in the competition process no matter which first precipitates. The anisotropic growth and coarsening of θ phase result in the preferred orientation microstructure in the coarsening process.

References

- [1] MOVERARE J J, JOHANSSON S, REED R C. Deformation and damage mechanisms during thermal–mechanical fatigue of a single-crystal superalloy [J]. *Acta Materialia*, 2009, 57: 2266–2276.
- [2] SALTUKONV P, FABRICHNAYA O, GOLCZEWSKI J, ALDINGER F. Thermodynamic modeling of oxidation of Al–Cr–Ni alloys [J]. *Journal of Alloys and Compounds*, 2004, 38: 99–113.
- [3] LU B L, CHEN G Q, QU S, SU H, ZHOU W L. First-principle calculation of yield stress anomaly of Ni_3Al -based alloys [J]. *Materials Science and Engineering A*, 2013, 565: 317–320.
- [4] LU Y L, ZHANG L C, CHEN Y P, CHEN Z, WANG Y X. Phase-field study for the pre-precipitation process of L_{12} - Ni_3Al phase in Ni–Al–V alloy [J]. *Intermetallics*, 2013, 38: 144–149.
- [5] NABARRO F R N, CRESS C M, KOTSCHY P. The thermodynamic driving force for rafting in superalloys [J]. *Acta Materialia*, 1996, 44: 3189–3198.
- [6] REED R C, COX D C, RAE C M F. Damage accumulation during creep deformation of a single crystal superalloy at 1150 °C [J]. *Materials Science and Engineering A*, 2007, 448: 88–96.
- [7] LI S, SU G T, TAO J. Influence of pre-compression on microstructure and creep characteristic of a single crystal nickel-base superalloy [J]. *Materials Science and Engineering A*, 2006, 418: 229–235.
- [8] WU Yu-xiao, ZHANG Heng, LI Fu-lin, LI Shu-suo, GONG Sheng-kai, HAN Ya-fang. Kinetics and microstructural evolution during recrystallization of a Ni_3Al -based single crystal superalloy [J]. *Transactions of Nonferrous Metals Society of China*, 2012, 22(9): 2098–2105.
- [9] MIYAZAKI T, KOYAMA T, KOZAKAI T. Computer simulations of the phase transformation in real alloy systems based on the phase field method [J]. *Materials Science and Engineering A*, 2001, 312: 38–49.
- [10] SHEN C, SIMMONS J P, WU K, WANG Y. Development of computational tools for microstructural engineering of Ni-based superalloys by means of the phase field method [C]//*Materials Design Approaches and Experiences*. Warrendale, PA: TMS, 2001: 57–74.
- [11] ZHAO Yan, CHEN Zheng, LU Yan-li, ZHANG Li-peng. Microscopic phase-field study on aging behavior of $\text{Ni}_{75}\text{Al}_{17}\text{Zn}_8$ [J]. *Transactions of Nonferrous Metals Society of China*, 2010, 20(4): 675–681.
- [12] ZHANG Ming-yi, LIU Fu, CHEN Zheng, GUO Hong-jun, YUE Guang-quan, YANG Kun. Site occupation evolution of alloying elements in L_{12} phase during phase transformation in $\text{Ni}_{75}\text{Al}_{7.5}\text{V}_{17.5}$ [J]. *Transactions of Nonferrous Metals Society of China*, 2012, 22(10): 2439–2443.
- [13] YANG Kun, ZHANG Ming-yi, CHEN Zheng, FAN Xiao-li. Microscopic phase-field study for mechanisms of directional coarsening and the transformation of rafting types in Ni–Al–V ternary alloys [J]. *Computational Materials Science*, 2012, 62: 160–168.
- [14] KHACHATURYAN A G. *Theory of structural transformation in solids* [M]. New York: Wiley, 1983: 129.
- [15] PODURI R, CHEN Long-qing. Computer simulation of the kinetics of order-disorder and phase separation during precipitation of δ' (Al_3Li) in Al–Li alloys [J]. *Acta Materialia*, 1997, 45: 245–255.
- [16] PODURI R, CHEN Long-qing. Computer simulation of atomic ordering and compositional clustering in the pseudobinary Ni_3Al - Ni_3V system [J]. *Acta Materialia*, 1998, 46: 1719–1729.
- [17] WANG Y, CHEN Long-qing, KHACHATURYAN A G. Shape evolution of a precipitate during strain-induced coarsening: A

- computer simulation [J]. Scripta Metallurgica et Materialia, 1991, 25: 1969–1974.
- [18] WANG Y, CHEN L Q, KHACHATURYAN A G. Kinetics of strain-induced morphological transformation in cubic alloys with a miscibility gap [J]. Acta Metallurgica et Materialia, 1993, 41: 279–296.
- [19] PRIKHODKO S V, CARNES J D, ISAAK D G, ARDELL A J. Elastic constants of a Ni–12.69%Al alloy from 295 to 1 300 K [J]. Scripta Metallurgica, 1998, 38: 67–72.
- [20] KANENO Y, SOGA W, TSUDA H, TAKASUGI T. Microstructural evolution and mechanical property in dual two-phase intermetallic alloys composed of geometrically close-packed Ni₃X (X: Al and V) containing Nb [J]. Journal of Materials Science, 2008, 43: 748–758.
- [21] CHENG K Y, JO C Y, KIM D H, JIN T, HU Z Q. Influence of local chemical segregation on the γ' directional coarsening behavior in single crystal superalloy CMSX-4 [J]. Materials Characterization, 2009, 60: 210–218.
- [22] TAKEYAMA M, KIKUCHI M. Eutectoid transformations accompanied by ordering [J]. Intermetallics, 1998, 6: 573–578.
- [23] MAEBASHI T, DOI M. Coarsening behaviours of coherent γ' and γ precipitates in elastically constrained Ni–Al–Ti alloys [J]. Materials Science and Engineering A, 2004, 373: 72–79.

相场方法研究 Ni–Al–V 合金的竞争沉淀过程

卢艳丽, 卢广明, 贾德伟, 陈 铮

西北工业大学 凝固技术国家重点实验室, 西安 710072

摘 要: 采用微观相场动力学模型, 在原子层面上研究 Ni₇₅Al_xV_{25-x} 合金中 γ' 相和 θ 相的沉淀过程及微观结构演化。模拟实验结果表明, Al 浓度对沉淀序列具有重要的影响。低 Al 浓度合金中, 先析出 θ (Ni₃V) 有序相, 随后析出 γ' (Ni₃Al) 有序相; 中 Al 浓度合金中, θ 有序相及 γ' 有序相几乎同时析出; 高 Al 浓度合金中, γ' 有序相先析出, θ 有序相随后析出。沉淀过程中, θ 有序相和 γ' 有序相长大和粗化过程中存在竞争关系, 无论先析出哪种相, θ 有序相在粗化的竞争过程中占有优势。因此, 沉淀最后形成择优取向的显微组织。

关键词: Ni–Al–V 合金; 微观结构演化; 沉淀过程; 相场方法

(Edited by Xiang-qun LI)